Rubber-Modified Glassy Amorphous Polymers Prepared via Chemically Induced Phase Separation. 3. Influence of the Strain Rate on the Microscopic Deformation Mechanism

B. J. P. Jansen, S. Rastogi,* H. E. H. Meijer, and P. J. Lemstra

Eindhoven Polymer Laboratories, Dutch Polymer Institute, Eindhoven University of Technology, PO Box 513, 5600 MB Eindhoven, The Netherlands

Received September 4, 1998; Revised Manuscript Received February 19, 1999

ABSTRACT: The mode of microscopic deformation during impact testing of a 80/20 PMMA/rubber blend has been examined by in situ small-angle X-ray scattering using synchrotron radiation. As discussed previously, the blend studied possesses an extremely small dispersed rubber phase prepared via chemically induced phase separation and responds as ductile during tensile deformation but suffers from brittle failure under impact conditions. In part 2, it was shown that the ductile behavior is accompanied by cavitation which relieves the triaxial stress state and, subsequently, promotes shear yielding. The present study demonstrates that increasing the strain rate leads to an enhancement of the nucleation of voids combined with a decreasing tendency for void orientation upon tensile deformation. By the introduction of a notch, the deformation rate is enhanced even further, and the mode of microscopic deformation transforms to crazing, which explains the poor macroscopic impact toughness. Precavitation of the samples, however, restores the toughness, even under impact conditions.

1. Introduction

The resistance against fracture and the ability to absorb a sudden impact are of crucial importance during the development of polymer blends. Therefore, both the composition and the morphology are carefully designed to achieve a maximum toughness at high deformation rates.[1,2] Special tests, such as falling weight tests or flexed-beam tests such as Izod and Charpy impact tests,[2] are used for the characterization of impact strengths. Test parameters such as sample geometry, experimental setups, and test rates are standardized (e.g., in ASTM or DIN).

The accuracy and reproducibility of both slow- and high-speed tensile deformation tests are generally higher and, therefore, often preferred in more fundamental studies. Due to differences in notch sensitivity, an improved tensile toughness does not always result in an enhanced impact strength. In the case of polycarbonate for example, the Izod impact strength can change by 1 order of magnitude for test specimens with sharp and blunt notches.[3] Another example is rubber-modified poly(methyl methacrylate) (PMMA) as used in this research, which demonstrates a strong increase in tensile toughness with increasing rubber content while the impact strength is not improved at all.[4] The enhanced ductility at limited deformation rates, found upon increasing the rubber content in this blend, is caused by the transition in mode of microscopic deformation from crazing to shear yielding as was shown by in situ small-angle X-ray scattering (SAXS) experiments during tensile deformation.[5]

Most of the earlier reported studies on real-time synchrotron deformation−SAXS are performed at limited strain rates[5−13] while only a few have been carried out under impact conditions.[14−16] In particular, in the latter case, the high intensity of the synchrotron source used is of crucial importance in order to follow deformation development at time resolutions less than one-hundredth of a second. Bubeck et al.[14] and Buckley[15] showed that the amount of crazing in high impact polystyrene (HIPS) and acrylonitrile−butadiene−styrene (ABS) decreases as the deformation rate in notched impact tests is increased. For polyethylene, Hughes et al.[16] successfully performed simultaneous small- and wide-angle X-ray scattering experiments during high-speed tensile deformation which is especially interesting in the study of deformation behavior of semicrystalline polymers.

This paper describes the influence of strain rate on the mode of microscopic deformation in the epoxy rubber-modified PMMA, which had been introduced earlier,[4,5] and focuses on the 80/20 blend.

2. Experimental Section

2.1. Materials. The PMMA rubber blends were prepared via chemically induced phase separation during the simultaneous polymerization of methyl methacrylate (MMA) and an aliphatic epoxy resin (SHELL Epikote 877) as discussed in more detail in the first paper of this series.[4] The size of the dispersed epoxy rubber phase was suppressed by controlling the system viscosity during phase separation.[4,17] In this study, one blend composition was considered: PMMA/epoxy 80/20, using the 90/10 composition as a reference.

2.2. Techniques. The small-angle X-ray (SAXS) experiments were performed at station 2.1 of the synchrotron facility at the CLRC (Daresbury Laboratories, Warrington, U.K.). The experimental setup used has been described in more detail in the previous paper of this series.[5]

The samples were stretched using a Rheometrics Minimat miniature tensile machine, which was tilted 45° from the vertical direction in order to avoid experimental errors as result of the rectangular beam spot. The tensile experiments were performed at different deformation rates varying between 0.01 and 25 mm/min using both notched and unnotched samples. Fresh notches were introduced using a scalping knife prior to testing.

The data were converted into absolute intensities in order to allow for a proper comparison of the scattering data collected at different strain rates. Calibration was performed using a

* To whom correspondence should be addressed.

10.1021/ma981406n CCC: $18.00 © 1999 American Chemical Society
Published on Web 09/03/1999

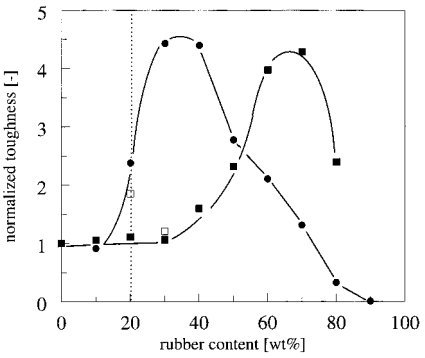

Figure 1. Tensile (●) and impact (■) toughness of the PMMA/epoxy blends normalized to neat PMMA vs the rubber content. Two blend compositions, 80/20 and 70/30, have been predeformed in tensile prior to impact testing (□).

polyurethane sample with known absorption coefficients.[18] The total beam intensity in front of and behind the sample was recorded by two ionization chambers during the complete drawing process.

2.3. Data Analysis. The method of analyzing the scattering and strain data has also been discussed in more detail before.[5] From the scattering data, the invariants parallel, $Q_{\parallel}$, and perpendicular, $Q_{\perp}$, to tensile direction are determined in order to visualize the development and extent of orientation during drawing. The absorption data collected by the ionization chambers are used to calculate the local strain in the beam spot. In this paper, we have refrained from calculation of the absolute void volumes on purpose, since most of the scattering, originating from voids, will be very close to the beamstop, a resolution limitation in terms of the SAXS setup we used. Further extrapolation of the intensity to the zero scattering angle, which is the main factor in a quantitative determination of the absolute void volume, was not very convincing, at least in our case.

3. Results and Discussion

3.1. Macroscopic Properties. The macroscopic properties of the PMMA/epoxy system are summarized in Figure 1. The tensile toughness is significantly improved at epoxy contents of 20 wt % and more, and the maximum value is found at 30−40 wt %. In contrast, under notched impact conditions, the toughness remains unimproved up to 30 wt % rubber while the maximum is shifted to a rubber content of 60−70 wt %. The ductility of the PMMA/epoxy 80/20 blend, which showed cavitation during tensile testing, is completely lost at higher deformation rates. To explain this in terms of microscopic deformation, in this study the strain rate dependence of the cavitation process will be investigated. The development of the voids is monitored at different strain rates using both unnotched and notched samples. Notches are applied to increase the local deformation rate.

3.2. Unnotched Samples. In parts a and b of Figure 2, the scattering patterns prior to fracture are shown for two unnotched samples, deformed at respectively 0.01 and 25 mm/min. It is evident from these patterns that the deformation for both strain rates is mainly accompanied by cavitation on a microscopic level. The formation of the voids and the development of the resulting scattering patterns have been discussed before.[5] Summarizing, cavitation relieves the triaxial stress state upon drawing, which promotes the occurrence of shear yielding. This results in high local strains of more than 150% which leads to orientation of the formed voids in the tensile direction. (The local strain is defined as the strain measured in the local region of the sample exposed by the X-ray beam. For the detailed calculation procedure, see part 2 of this series.[5])

The observed elliptically shaped scattering patterns are attributed to these highly oriented voids. Apparently, the mode of microscopic deformation does not change with increasing strain rate, in the range investigated. Next, the results at different intermediate strain rates will be discussed in more detail.

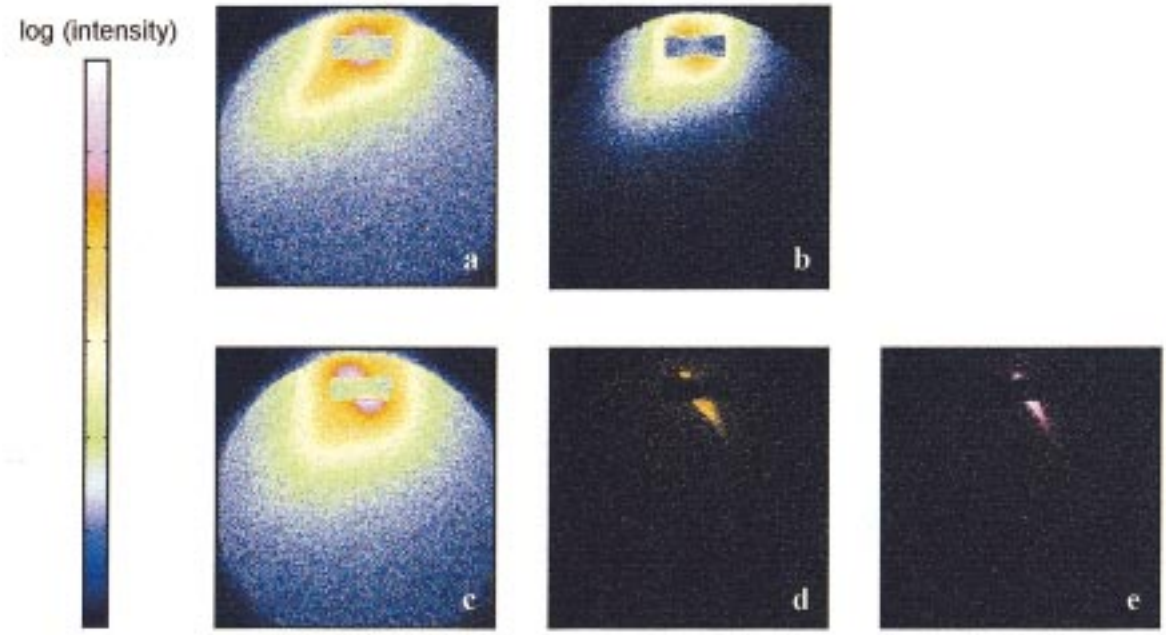

Figure 2. Small-angle X-ray scattering patterns of the PMMA/epoxy 80/20 blend prior to fracture, deformed at (a) 0.1 and (b) 25 mm/min. Scattering patterns for notched samples of the same blend stretched at (c) 0.01 and (d) 25 mm/min. (e) Pattern measured for a notched PMMA/epoxy 90/10 sample tested at 25 mm/min. The tensile direction is tilted 45°, "counterclockwise". Experiments performed at CLRC, Station 2.1.

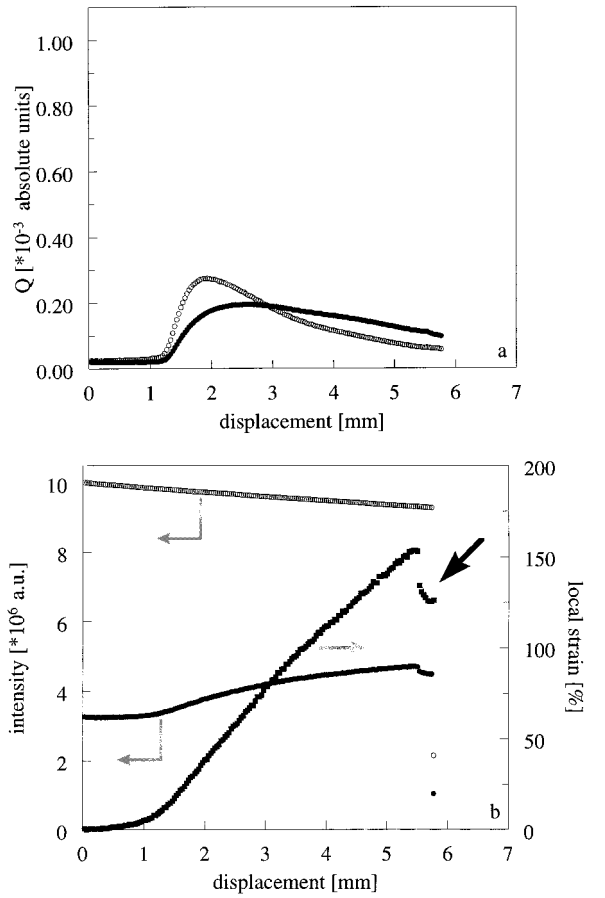

Figure 3. SAXS data for the in situ deformation of unnotched PMMA/epoxy 80/20 at a displacement rate of 0.1 mm/min: (a) absolute invariant perpendicular (●) and parallel (○) to the tensile direction vs the clamp displacement; (b) local strain (■), intensity of the first (○) and second (●) ionization chamber vs clamp displacement.

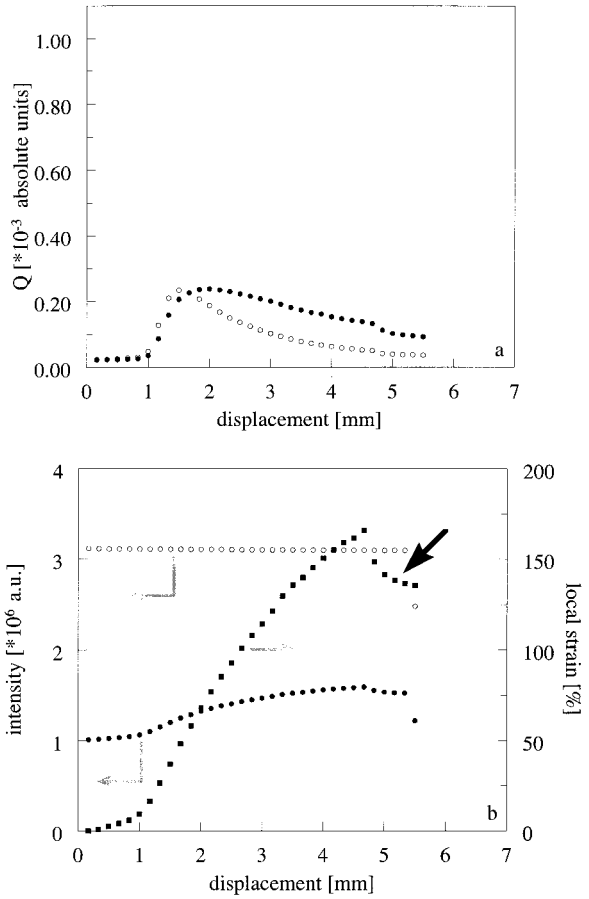

Figure 4. As in Figure 3, for a displacement rate of 1 mm/min.

3.2.1. 0.1 mm/min. As can be observed in Figure 3a, the invariants in both principal directions show a sudden increase at a displacement of approximately 1 mm. The strong scattering is the result of a sudden enhancement in the electron density difference caused by the onset of void formation. Initially, the scattering in the tensile direction is higher than in the perpendicular direction. This indicates the formation of cracklike voids or the introduction of some crazes, which both cause relatively more scattering in the tensile direction.[19,20] The voids thus formed are elongated during further drawing, which results in a redistribution of the scattered intensity over both principal directions. Eventually, the perpendicular invariant starts to exceed the parallel invariant at higher draw ratios as expected from the development of the observed elliptical-shaped scattering pattern. The overall decrease of the invariants is caused by the decreasing amount of scattering units in the beam due to sample thinning at higher strains.

As expected, the onsets of both the local strain and scattering occur simultaneously and is observed at a displacement of approximately 1 mm; compare parts a and b of Figure 3. As a result of the sample geometry, the exact strain rate cannot be controlled but can be estimated from the slope of the local strain vs the clamp displacement, which is equivalent to the deformation time. Although the clamp displacement rate is constant (0.1 mm/min), the local strain rate appears to decrease slowly toward the end of the tensile test. The sudden decrease in local strain, indicated by the arrow in Figure 3b, is explained by a crack initiation outside the beam spot, which allows a partial relieve of the elastic strain. Due to the resulting increase in the sample thickness, local absorption of radiation is enhanced.

3.2.2. 1 mm/min. Figure 4 shows the results at a displacement rate of 1 mm/min. If the deformation rate is increased by 1 order of magnitude, a similar development of both invariants is observed; compare Figures 3a and 4a. Again the introduction of voids causes a sudden increase in scattering intensity. The volumes of voids for both strain rates appear to be identical since the value of the invariants is approximately the same. However, increasing the strain rate decreases the relative difference between the invariants for both directions which indicates the formation of more isotropic voids. Less cracklike voids and/or crazes seem to be formed as can be concluded from the relatively decreased amount of scattering in the tensile direction. Due to the void elongation at higher strains, the perpendicular invariant starts again to exceed the parallel invariant.

The local strain is also hardly affected by the increasing strain rate; compare Figures 3b and 4b. The strain developments are similar, and at a higher deformation the drop in local strain due to crack initiation prior to fracture is again clearly visible; see the arrow in Figure 4b. As expected, the slope of the local strain curve is steeper in Figure 4b, which indicates that the local strain rate increases with the displacement rate of the clamps.

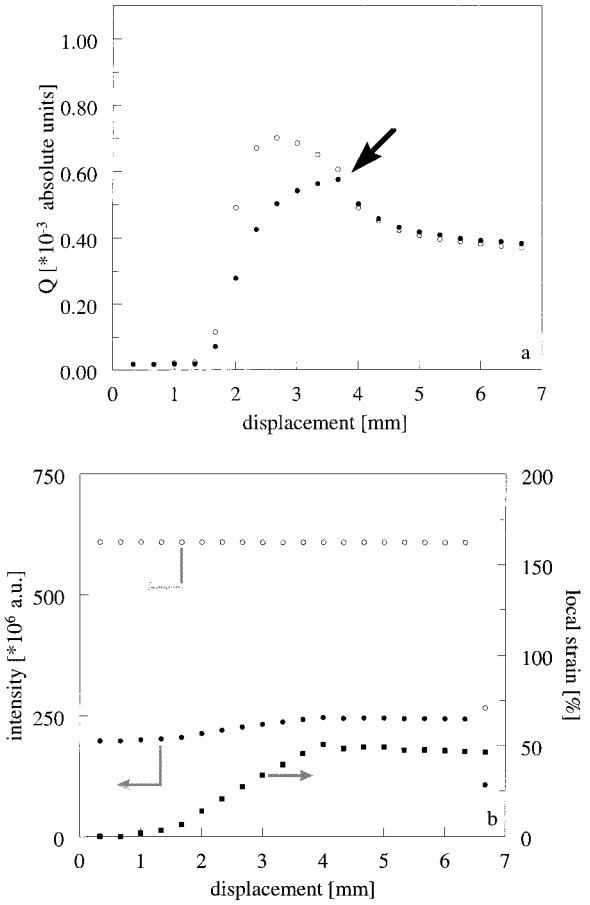

Figure 5. As in Figure 3, for a displacement rate of 10 mm/min.

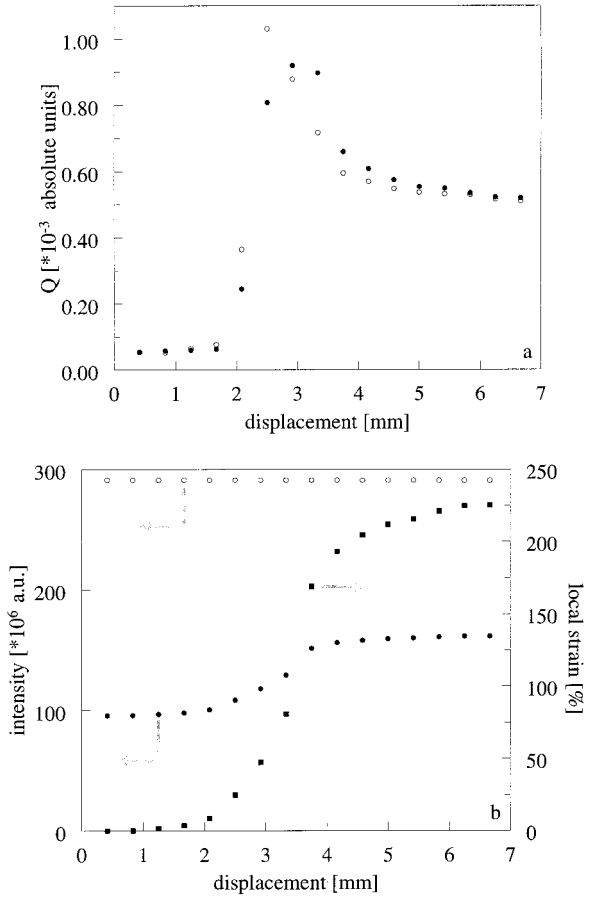

Figure 6. As in Figure 3, for a displacement rate of 25 mm/min.

3.2.3. 10 mm/min. If the deformation rate is increased to 10 mm/min, the quantitative values of the invariants increase by a factor of 3; compare Figures 4a and 5a. This suggests increasing amounts of voids and/or void volume. The initial difference between the invariants for both principal directions suddenly disappears at a displacement of almost 4 mm. The value of the invarants become equal as a result of an abrupt change in the perpendicular invariant as indicated by the arrow in Figure 5a.

Unlike the measurements at lower deformation rates, Figures 3b and 4b, here the local strain shows a sudden change at a displacement of 4 mm and becomes constant for the remaining deformation, Figure 5b. Moreover, for this particular experiment the increase in deformation rate to 10 mm/min does not result in the expected enhancement of the local strain rate, as can be concluded from the limited slope of the curve; compare Figures 3b, 4b, and 5b. In conclusion, the data collected at this strain rate should be carefully interpreted since the invariant and local strain data suggest a rather inhomogeneous deformation behavior of the material in the beam spot.

3.2.4. 25 mm/min. Unlike the experiments performed at a displacement rate of 10 mm/min, Figure 6 suggests a homogeneous local deformation at 25 mm/min. Figure 6a shows a very strong and abrupt increase of the invariants at a displacement of 2 mm. The reason is most likely again the occurrence of cavitation, which introduces a large difference in electron density. The amount of cavitation clearly increases with increasing strain rate as can be concluded from the comparison of the absolute invariants with those of the experiments discussed above. The maxima in the invariants are again the result of sample thinning. From a displacement of 5 mm onward, both invariants become equal as result of a similar electron density fluctuation along the principal directions. This indicates that on average the voids are less oriented along the tensile direction, in contrast to the observations at lower deformation rates, see for an example Figure 3a. This is confirmed by the decrease in the aspect ratio of the elliptical shaped scattering pattern at higher deformation rates, compare Figures 2a and b.

The development in local strain in Figure 6b occurs in the same displacement regime as the observed changes in scattering intensity; compare parts a and b of Figure 6. The maximum slope of the curve is relatively steep, which is evidence for a high local strain rate. Moreover, the strain at break is extremely high, more than 200%, and exceeds that of the tests performed at lower strain rates. In contrast to the lower deformation rates, no fracture is detected within the same displacement region. Moreover, beyond 5 mm, no increase in local strain is observed, indicating that the deformation occurs outside the region exposed by the incident X-ray beam.

From the development in invariants and local strain measured at different deformation rates, a few general conclusions can be drawn. The absolute values of the invariants suggest that cavitation is enhanced at higher strain rates. At limited rates, deformation starts with cavitation, which is followed by a strong orientation in the tensile direction of the voids formed. This explains

the development of the elliptical scattering pattern and the resulting differences in scattering intensity between both directions. In contrast, higher rates seem to promote the nucleation of additional voids instead of the orientation of voids which are formed during the early stage of the cavitation process. This is concluded from the fact that the absolute values of the invariants are enhanced with increasing strain rates while the differences between both principal scattering directions are suppressed.

3.3. Notched Samples. For the experiments discussed above, no transition in the mode of microscopic deformation is observed at higher strain rates. Nevertheless, the macroscopic mechanical behavior of the PMMA/epoxy 80/20 blend changes to brittle for impact conditions. Since 25 mm/min is the maximum displacement rate of the stretching device used, notches are introduced in the test samples. They will generate an additional increase in the local deformation rate behind the notch.

3.3.1. PMMA/Epoxy 80/20. Parts c and d of Figure 2 show the scattering patterns of the deformed zone behind the notch in the PMMA/epoxy 80/20 blend. A displacement rate of 0.01 mm/min (Figure 2c) does not result in a transition in deformation behavior in comparison to that of the unnotched samples. The strong scattering pattern is again caused by the formation of voids. However, the aspect ratio of elliptical shape is decreased, which suggests a limited elongation of these voids upon further drawing. Moreover, the combination of the elliptical SAXS pattern and the enhanced scattering in the tensile direction should be the result of inhomogeneous deformation in the region exposed by the beam spot. This is not surprising considering the limited size of the deformation zone behind a notch and the experimental setup, i.e., the orientation of the beam relative to the sample coordinates. As a result of the inhomogeneous deformation, the invariant in the tensile direction in Figure 7a remains higher than the perpendicular invariant during the complete drawing process. The maximum observed is again caused by sample thinning due to shear yielding, which is promoted by the introduction of the voids. Despite the differences observed, the mode of microscopic deformation in a notched sample at limited strain rate is identical to that in a uniaxial tensile test without notch, i.e., cavitation-induced shear yielding.

Increasing the displacement rate to 25 mm/min in notched samples causes a dramatic change in scattering pattern; see Figure 2d. The void scattering is replaced by only one single but strong streak in the tensile direction, without the occurrence of any scattering in the perpendicular direction. Moreover, the corresponding perpendicular invariant in Figure 7b remains constant over the course of time during the complete deformation process. The scattering of the streak gives rise to a sudden stepwise increase for the invariant in the tensile direction. However, a measuring resolution of 25 ms appears to be insufficient to collect data points during its development. The most plausible explanation for the observed streak is the introduction of crazes as the electron density difference between the craze−bulk and polymer matrix is known to give rise to a very strong scattering in the tensile direction.[19,20] However, in contrast to these results, the scattering of craze fibrils in the perpendicular direction is usually also observed and can be used to determine the total amount of strain

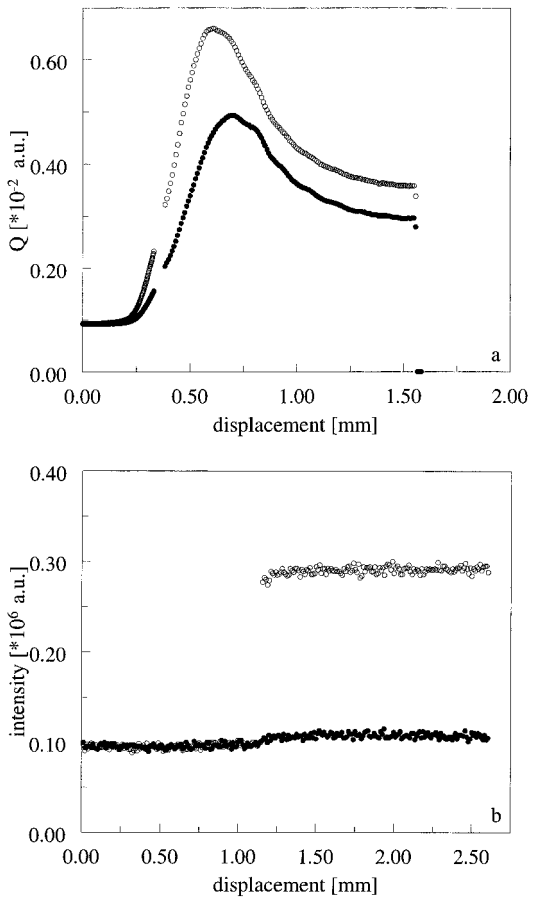

Figure 7. Invariant perpendicular (●) and parallel (○) to the tensile direction vs the clamp displacement for the in situ deformation of a notched PMMA/epoxy 80/20 blend at displacement rates of (a) 0.01 and (b) 25 mm/min.

related to the crazing process.[14,15] The absence of this scattering suggests the formation of only a small amount of craze volume and/or crazes with a limited fibril content as result of the elevated local strain rate.

3.3.2. PMMA/Epoxy 90/10. The occurrence of crazing and the resulting scattering pattern for the PMMA/epoxy 80/20 blend is verified by applying the same test conditions for a 90/10 blend. This blend is brittle and exhibits crazing even at limited strain rates without notching.[5] The craze scattering patterns during slow-speed tensile testing include the expected fibril scattering in the perpendicular direction which was used to calculate the craze−fibril diameter. More extreme testing conditions result again in only a single scattering streak in the tensile direction as was observed for the PMMA/epoxy 80/20 blend; see parts d and e of Figure 2. Consequently, the mode of deformation does not appear to change for the 90/10 blend with increasing strain rate since the scattering patterns observed at both slow- and high-speed testing are attributed to crazing. However, the type, size and/or amount of the crazes involved appears to be influenced by the strain rate, considering the differences in the craze scattering patterns. Since for the PMMA/epoxy 90/10 blend crazing is expected, the similarity between the scattering patterns of the 90/10 and 80/20 blend further confirms the occurrence of crazing for the latter blend at higher strain rates. Consequently, it can be concluded that the mode of microscopic deformation for the PMMA/epoxy 80/20 blend transforms from cavitation induced shear yielding

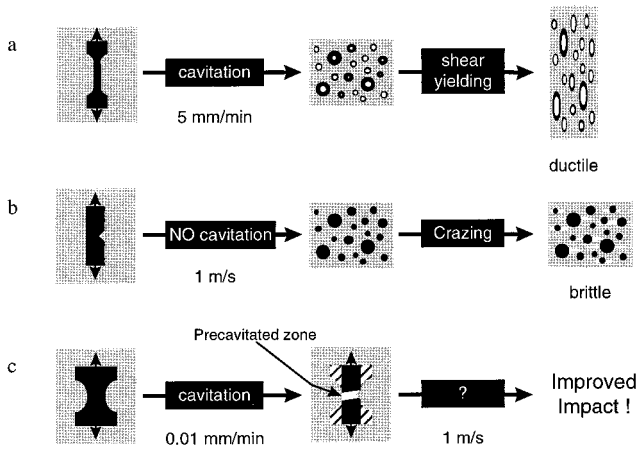

Figure 8. Schematic representation of the relation between the mechanical test, the mode of microscopic deformation determined via the in situ SAXS measurements and the macroscopic toughness of the PMMA/epoxy 80/20 blend: (a) tensile, (b) impact deformation, and (c) a combined test in which a sample is predeformed in the tensile test prior to impact testing.

to crazing by shifting the testing condition from tensile to impact.

3.4. Macroscopic vs Microscopic Deformation. As discussed, the maximum macroscopic toughness of the PMMA/epoxy blends shifts to higher epoxy concentrations by changing the test conditions from tensile to impact. For the PMMA/epoxy 80/20 blend the impact toughness is equal to that of neat PMMA while the tensile toughness is significantly improved. The in situ SAXS−deformation experiments demonstrate that this is accompanied by a transition in mode of microscopic deformation. In Figure 8 the macroscopic performance and the relating microscopic deformation of the PMMA/epoxy 80/20 blend are summarized. During slow speed tensile testing, cavitation will relieve the triaxial stress state which, subsequently, promotes shear yielding upon further drawing.[21,22] This will enhance the ductility of the blend and thus its tensile toughness; see Figure 8a. Since cavitation apparently cannot, or can hardly, occur during impact deformation, crazing rather than shear yielding occurs, which causes a brittle behavior and, therefore, a limited impact toughness; see Figure 8b. However, the influence of void formation on the impact behavior can easily be studied by a combination of tensile and impact testing. First, dumbbell-shaped samples are predeformed at a limited strain rate in order to induce cavitation in the stress concentration zone; see Figure 8c. During the predeformation process, the yield stress is first passed and, subsequently, followed by an additional deformation of a few percent. Next, the samples are shaped into Izod impact bars for which the notch is machined in the precavitated zone. The impact toughness of the PMMA/epoxy 80/20 blends increases substantially by following this precavitation procedure; see the open squares in Figure 1. In conclusion, cavitation promotes shear yielding also under impact conditions and thus improves the impact strength. This is confirmed by similar predeformation experiments for the PMMA/epoxy 70/30 blend. As expected, the impact toughness is hardly improved since cavitation does not occur during predeformation of this blend.[5] The limited toughness enhancement observed in Figure 1 is most probably the result of orientation.

The resistance against cavitation is known to increase with decreasing particle size.[23−25] Hence, this is expected to be of importance especially in case of the submicrometer- to nanometer-sized morphologies of the PMMA/epoxy 80/20 blend. However, this does not explain the apparent strain rate dependence of the cavitation process. An alternative reason can be found in the strain rate dependence of the rubber modulus.[23,26,27] At very high rates the modulus of the dispersed rubber phase may approach that of a glass, which will promote its resistance against cavitation.[26] As a result, cavitation and thus shear yielding, is suppressed during impact deformation, which explains the brittle failure found.

4. Conclusions

The improved toughness of a PMMA/epoxy 80/20 blend during tensile deformation is lost under impact conditions. To explain this finding, the changes in microscopic deformation of this blend are studied by means of real-time SAXS−deformation experiments.

During uniaxial tensile testing at limited strain rate, shear yielding is promoted by the occurrence of cavitation, which causes a ductile macroscopic behavior. At higher deformation rates the volume of voids formed increases while the degree of orientation of these voids in the tensile direction after formation decreases. Apparently, the nucleation of new voids is enhanced by a higher rate while deformation at limited rate more predominantly occurs via the orientation of voids which are formed in an early stage of the drawing process.

By the introduction of a notch, the strain rate is enhanced which results in a transition from cavitation induced shear yielding to crazing. This is in accordance with the macroscopic mechanical behavior of the blend, which becomes brittle under impact conditions.

The relation between the strain rate and the degree of the cavitation of the PMMA/epoxy 80/20 seems to possess an optimum value. First, the tendency for cavitation is enhanced by the higher strain rate, which would suggest an additional toughness improvement at macroscopic level. However, at even higher rates, void formation can no longer occur, causing brittle failure. Apparently, cavitation is a prerequirement for this blend to behave ductile at a macroscopic level. This is confirmed by the enhanced impact strength of the PMMA/epoxy 80/20 system, which is precavitated during slow speed tensile deformation prior to impact testing.

Generally, the toughness of brittle amorphous polymers can be improved by a transition in mode of microscopic deformation from crazing to shear yielding. To achieve this, one should aim for a smaller but more readily cavitating dispersed rubber phase.

Acknowledgment. The authors wish to thank Prof. A. J. Ryan and Dr. P. Fairclough (University of Sheffield, Sheffield, U.K.) and Dr. N. Tyrell and Dr. A. Gleeson (SRS, CLRC, Warrington, U.K.) for the availability of the X-ray facilities at station 2.1 of the at the Synchrotron Radiation Source (SRS, Warrington, U.K.) and their experimental contributions.

References and Notes

(1) Bucknall, C. B. *Toughened Plastics*; Applied Science Publishers Ltd.: London, 1977.
(2) Kinloch, A. J.; Young, R. J. *Fracture Behavior of Polymers*; Elsevier Applied Science Publishers Ltd.: London, 1983.
(3) Plati, E.; Williams, J. G. *Polym. Eng. Sci.* **1975**, *8*, 941.
(4) Part 1. Jansen, B. J. P.; Meijer, H. E. H.; Lemstra, P. J. *Polymer*, submitted for publication.

(5) Part 2. Jansen, B. J. P.; Rastogi S.; Meijer, H. E. H.; Lemstra, P. J. *Macromolecules*, submitted for publication.
(6) He, C.; Donald, A. M.; Butler, M. F.; Diat, O. *Polymer* **1998**, *39*, 659.
(7) He, C.; Donald, A. M.; Butler, M. F. *Macromolecules* **1998**, *31*, 158.
(8) Lovell, P. A.; Ryan, A. J.; Sherratt, M. N.; Young, R. J. *Polym. Mater. Sci. Eng.* **1994**, *70*, 155.
(9) Ijichi, Y.; Kojima, T.; Suzuki, Y.; Nishio, T.; Kakugo, M. *Macromolecules* **1993**, *26*, 829.
(10) Okamoto, Y.; Miyagi, H.; Uno, T.; Amemiya, Y. *Polym. Eng. Sci.* **1993**, *33*, 1608.
(11) Butler, M. F.; Donald, A. M.; Ryan, A. J. *Polymer* **1997**, *38*, 5521.
(12) Butler, M. F.; Donald, A. M.; Ryan, A. J. *Polymer* **1997**, *39*, 781.
(13) Butler, M. F.; Donald, A. M.; Bras W.; Mant, G. R.; Derbyshire, G. E.; Ryan, A. J. *Macromolecules* **1995**, *28*, 6383.
(14) Bubeck, R. A.; Buckley, D. J.; Kramer; Brown, H. R. *J. Mater. Sci.* **1991**, *26*, 6249.
(15) Buckley, D. J., Jr. Ph.D. Thesis, Cornell University, 1993.
(16) Hughes, D. J.; Mahendrasinngam, A.; Oatway, W. B.; Heeley, E. L.; Martin, C.; Fuller, W. *Polymer* **1997**, *38*, 6427.
(17) Jansen, B. J. P.; Meijer, H. E. H.; Lemstra, P. J. *Polymer* **1999**, *40*, 2917.
(18) Kratky, O.; Pilz, I.; Schmitz, P. J. *J. Colloid Interface Sci.* **1966**, *21*, 24.
(19) Paredes, E.; Fischer, E. W. *Macromol. Chem.* **1979**, *180*, 2707.
(20) Brown, H. R.; Kramer, E. J. *J. Macromol. Sci.—Phys.* **1981**, *B19*, 487.
(21) Pearson, R. A.; Yee, A. F. *J. Mater. Sci.* **1991**, *26*, 3828.
(22) Bagheri, R.; Pearson, R. A. *Polymer* **1996**, *37*, 4529.
(23) Lazzeri, A.; Bucknall, C. B. *Polymer* **1995**, *36*, 2895.
(24) Cho, K.; Gent, A. N. *J. Mater. Sci.* **1988**, *26*, 141.
(25) Dompas, D.; Groenincks, G. *Polymer* **1994**, *35*, 22, 4743.
(26) Smit, R. J. M. Ph.D. Thesis, Eindhoven University of Technology, 1998.
(27) Smit, R. J. M.; Meijer, H. E. H.; Brekelmans, W. A. M.; Govaert, L. E. *J. Mater. Sci.* **1998**, submitted for publication.

MA981406N